

Article

Impacts of Rainfall Characteristics and Slope on Splash Detachment and Transport of Loess Soil

June Liu ^{1,*}, Fangyue Du ¹, Xike Cheng ¹, Xiaoqian Qi ¹, Ning Wang ¹, Nan Shen ², Chunyan Ma ³ and Zhanli Wang ²

¹ School of Geography and Tourism, Shaanxi Normal University, Xi'an 710119, China; dfy1253362810@snnu.edu.cn (F.D.); chengxike1117@163.com (X.C.); qxq@snnu.edu.cn (X.Q.); nzwang123456@snnu.edu.cn (N.W.)

² State Key Laboratory of Soil Erosion and Dryland Farming on the Loess Plateau, Institute of Soil and Water Conservation, Northwest A&F University, Xianyang 712100, China; shennan@nwsuaf.edu.cn (N.S.); zzwang@nwsuaf.edu.cn (Z.W.)

³ Shaanxi Key Laboratory of Ecological Restoration in Shaanbei Mining Area, Yulin University, Yulin 719000, China; nldmcy@yulinu.edu.cn

* Correspondence: liujune5@snnu.edu.cn; Tel.: +86-029-8531-0525

Abstract: To identify the key parameters and develop accurate experimental models of detachment and transport, splash detachment and transport of loess soil were investigated in relation to the rainfall characteristics and slope. The experiment was conducted under 25 combinations of five rainfall intensities (60, 84, 108, 132 and 156 mm h⁻¹) and five slope gradients (0°, 5°, 10°, 15° and 20°), using a custom splash pan. Raindrop characteristics (diameter, velocity and kinetics) and splash mass were measured in downslope and upslope. The results indicated that rainfall intensity and slope contributed 94.77% and 0.46%, respectively, to the detachment rate, and 24.39% and 67.82%, respectively, to the transport rate. From a holistic viewpoint, the positive effect of slope became more visible on the detachment rate when the rainfall intensity exceeded 108 mm h⁻¹, and on the transport rate when the slope exceeded 15°. Based on the rainfall simulator in this study, the rainfall kinetic energy (KE , J), raindrop median particle size (D_{50} , mm) and raindrop terminal velocity (V , m s⁻¹) all increased with increasing rainfall intensity (I) within the 60~108 mm h⁻¹ range but decreased with increasing rainfall intensity within the 132~156 mm h⁻¹ range. The rainfall intensity and raindrop characteristics ($D_{50}/V/KE$) are the key parameters of splash detachment (D_r , g·m⁻² min⁻¹), and three detachment models were developed: (1) $D_r = 0.1153 I^{1.09} D_{50}^{0.79}$ ($R^2 = 0.99$, $NSE = 0.98$, $p < 0.01$); (2) $D_r = 0.0162 I^{1.11} V^{1.22}$ ($R^2 = 0.99$, $NSE = 0.99$, $p < 0.01$); and (3) $D_r = 0.0813 I^{1.10} KE^{0.18}$ ($R^2 = 0.99$, $NSE = 0.99$, $p < 0.01$). The rainfall intensity and slope are the key parameters for splash transport (T_r , g·m⁻² min⁻¹), and the developed transport models could be expressed as: (1) $T_r = 0.00657 I^{1.343} S^{0.116}$ ($R^2 = 0.914$, $NSE = 0.874$, $p < 0.01$) (slopes of 0°, 5° and 10°) and (2) $T_r = 0.00218 I^{1.165} S^{1.033}$ ($R^2 = 0.986$, $NSE = 0.986$, $p < 0.01$) (slopes of 15° and 20°). The results of this study could enhance the understanding of soil splash detachment and transport on loess slopes.

Keywords: splash erosion; contribution rate; rainfall intensity; splash model; raindrop energy



Citation: Liu, J.; Du, F.; Cheng, X.; Qi, X.; Wang, N.; Shen, N.; Ma, C.; Wang, Z. Impacts of Rainfall Characteristics and Slope on Splash Detachment and Transport of Loess Soil. *Land* **2024**, *13*, 189. <https://doi.org/10.3390/land13020189>

Academic Editors: Vlassios Hrisanthou and Konstantinos Kaffas

Received: 30 December 2023

Revised: 31 January 2024

Accepted: 3 February 2024

Published: 5 February 2024



Copyright: © 2024 by the authors. Licensee MDPI, Basel, Switzerland. This article is an open access article distributed under the terms and conditions of the Creative Commons Attribution (CC BY) license (<https://creativecommons.org/licenses/by/4.0/>).

1. Introduction

Splash erosion is the first soil erosion process induced by rainfall and notably influences the overall erosion by removing surface soil material and transporting massive amounts of soil particles, which provides the material basis for soil erosion [1–3]. This complex process involves the detachment and transport of soil fragments due to raindrop impact [4]. At the beginning of a rainfall event, raindrops with a certain kinetic energy (KE) strike the soil surface. This leads to a breakdown of the soil structure, with soil particles dispersed and stripped from the soil body, resulting in a reduction or blockage of the soil surface pore space. This process is referred to as splash detachment [4]. The soil particle

transport phase is characterized by raindrops with sufficient kinetic energy to move particles along the slope when soil aggregates reach a certain particle size and weight, after which splash transport occurs [5,6]. Thus, detachment and transport during splash erosion are related mainly to the raindrop characteristics and ground slope [2,7–11], along with soil conditions (soil type, soil texture and structure, void fraction, stiffness and strength) [12].

The rainfall characteristics mainly include factors such as the rainfall intensity, rainfall kinetic energy, raindrop diameter and raindrop terminal velocity [13,14]. The impact of raindrops on splash erosion is mainly reflected in the number and energy of raindrops striking the soil surface. The rainfall intensity represents the number of raindrops received by the soil surface. The rainfall kinetic energy represents the energy of raindrops striking the soil surface and is largely determined by the raindrop diameter and velocity. With increasing rainfall intensity, the number of raindrops striking the surface soil increases, resulting in more soil particles fragmented and destroyed, producing more loose particulate matter to provide a basis for splash transport [15,16]. The rainfall kinetic energy acts on the surface and influences the soil, causing the disruption of soil aggregates and soil particles to easily leave the soil body, while the raindrop kinetic energy causes soil permeability changes, thus affecting the stability of runoff and enhancing the transport capacity of runoff [5,17]. As a significant topographic factor, the influence of the slope on splash erosion is mainly reflected in the variability of the gravitational action of soil particles on different surfaces [18,19]. With increasing slope, the gravitational component of the moving soil particles increases, the tendency of the soil particles to leave the soil body increases, and accordingly, the slope detachment mass increases. In addition, with increasing slope, the friction between the soil particles on the slope and the surface soil decreases, and the bond between the soil particles is reduced, which facilitates transport under the effect of raindrop splashing [20,21].

Many scholars have obtained constructive modelling results regarding the relationship between splash detachment and transport considering rainfall characteristics and slopes. The rainfall characteristics (rainfall intensity, raindrop kinetic energy, raindrop diameter, raindrop terminal velocity, etc.) all positively affected detachment and transport. However, different rainfall parameters were chosen for different splash detachment and transport models.

Regarding splash detachment, it has been argued that the most influential factor of splash erosion is the rainfall intensity, and only the rainfall intensity has been considered in detachment modelling, ignoring the slope factor [5,9,10,22–25]. Most of the models developed considering detachment and the rainfall intensity involve linear and power functions [5,9,10,22,24,25]. Several researchers have suggested that the rainfall intensity slightly affects detachment, and detachment models have been established based only on the slope, with both the slope and detachment indicating positive effects [26–28]. However, some results show that disengagement linearly increases with slope when the slope is less than 30° but decreases when the slope exceeds 30° [28]. In addition, it has been suggested that the rainfall intensity and slope are equally important for detachment, and the variation in the detachment rate with rainfall intensity and slope has been described by logarithmic and power function models [11,29]. The rainfall kinetic energy is considered more appropriate for describing the effect of rainfall on splash detachment. Scholars have considered only the kinetic energy of rainfall when modelling detachment, and the main model forms are power and linear functions [22,25,30,31]. Other scholars have combined the rainfall kinetic energy and slope to develop a power function model, where the index value of the rainfall kinetic energy is slightly higher than that of the slope [26]. In addition, the relationship between splash detachment and the kinetic energy of rainfall has been investigated by considering the raindrop diameter [11,32].

In terms of splash transport, it has been argued that the effect of the slope on transport is not significant, but slope factors have not been considered in transport modelling. Furbish et al. [33,34] suggested that the slope could contribute to the transport in both particle quantity and distance, and their proposed formula (raindrop momentum and its

distribution) reflected the average downslope displacement of grains increased with slopes as a weakly nonlinear function, although it was effectively linear up to 30° . Models relating the rainfall intensity and transport have been developed in power function and logarithmic forms [10,35]. Some researchers have not considered the rainfall intensity when modelling transport [27,30]. Very few scholars have considered the effects of both the rainfall intensity and slope during transport modelling, using sandy loam and silty loam soils for different ranges of the rainfall intensity and slope, with rainfall intensity index values close to 2 and slope index values close to 0.9 [36,37]. The effects of the rainfall kinetic energy and rainfall median particle size on transport have also been considered to model transport [27,34].

In summary, the relationship between rainfall characteristics and slope during splash detachment has been extensively modelled, but relatively little splash transport modelling has been performed. Regarding the combined effect of rainfall and slope on splash detachment and transport, different parameters have been selected to construct models. How to choose more reasonable and appropriate parameters to build a model should be studied further. In particular, there is no unified conclusion regarding the contributions of rainfall and slope to both detachment and transport. The aims of this study were to i) specify the effects of the rainfall intensity and slope on detachment and transport and their individual contributions through indoor simulated rainfall tests, and to ii) identify the key parameters to establish individual models of detachment and transport as affected by rainfall characteristics and slope.

2. Materials and Methods

2.1. Sampling Site and Soil

The study site located in Ansai County, Shaanxi Province, China ($109^\circ 19' \text{ E}$, $36^\circ 51' \text{ N}$), which is a typical loess hilly gully area. The average altitude of the area is approximately 1200 m. The average annual precipitation is about 500 mm, more than 60% of which occurs mostly in high-intensity rainstorms and primarily from July to September [11,38]. The topography of Ansai is characterized by high mountains, steep slopes and deep ditches, with low terrain in the southeast and high terrain in the northwest. Jungle grassland is the main vegetation type in the central part of Ansai, while sandy vegetation is the main vegetation type in the northern part of Ansai. The soil is a typical loess soil commonly encountered on the Loess Plateau and is relatively erodible [38]. The Loess Plateau hosts a soil erosion area of approximately 430,000 km², accounting for approximately 75% of the total area [39], and the area with a soil erosion modulus above 5000 t·km⁻² a⁻¹ amounts to 156,000 km².

Test soil was collected at a depth ranging from 0~25 cm in the cultivated layer of an agricultural field and comprised 32.88% sand (diameter: 0.05~2.0 mm), 61.17% silt (diameter: 0.002~0.05 mm) and 5.95% clay (diameter: <0.002 mm). Therefore, the test soil is a silty loam according to the USDA soil texture classification system, and belongs to Regosols according to World Reference Base for Soil Resources. The soil is poorly aggregated with an average diameter of 0.039 mm and composed of 0.5% organic matter. The saturated hydraulic conductivity is 0.59 mm min⁻¹. All the soil samples were pretreated by passing through a 10-mm sieve to remove debris such as small stones and plant residues, followed by air-drying.

2.2. Experimental Equipment

2.2.1. Simulated Rainfall Device

The experiments were conducted in the Simulation Rainfall Hall operated by the State Key Laboratory of Soil Erosion and Dryland Farming on the Loess Plateau in Yangling, Shaanxi Province, China. A rainfall simulator system with nozzles on two sides was used to reproduce simulated rainfall [40]. The rainfall simulator comprises an artificial rainfall simulator nozzle and a water measuring device. By varying the water pressure and nozzle size, the rainfall simulator can provide a rainfall intensity ranging from 10~220 mm h⁻¹. The rainfall intensity in this study ranged from 60~156 mm h⁻¹. The height of the side

spray simulator is 16 m, a height allowing most raindrops to reach the final velocity. The raindrop diameters range from 0.125~6.0 mm; moreover, their kinetic energy ranges from 2.63×10^{-10} ~ 4.99×10^{-4} J. In addition, the rainfall simulator achieved a uniformity higher than 80%.

2.2.2. Splash Pan

The splash pan used in this study was modified from the Morgan soil pan [41], which is constructed of stainless steel and exhibits a radius of 900 mm and a height of 100 mm. At the center of the pan, there is a soil sample pan with a radius (r) of 100 mm and a height of 100 mm, with small holes at the bottom for rainwater infiltration. A baffle divides the designed splash pan into upslope and downslope compartments (Figure 1), allowing separate measurement of the upslope and downslope splash amounts. Tap water (electrical conductivity = 0.7 dS m^{-1}) was used in all the experiments. To prevent the soil from escaping through the small holes in the splash pan, the bottom of the pan was covered with 1~2 layers of gauze before filling. Before test soil packing, the soil moisture content was adjusted to 14%, which is the typical level during the flood season on the Loess Plateau when most erosion events occur [38]. A bulk density of 1.2 g cm^{-3} (measured with a cutting ring in a compacted state) was adopted in this study, which is consistent with the in situ values. The samples were scraped flat and placed at the center of the splash pan. At the bottom of the splash pan, there are several 5-mm holes connected to a pipe for splash particle collection. Additionally, to ensure that only the source soil is affected by rainfall, a plastic cover with a 100-mm hole at the center was placed over the device. The slope gradient of the splash pan could be adjusted between 0% and 35%.

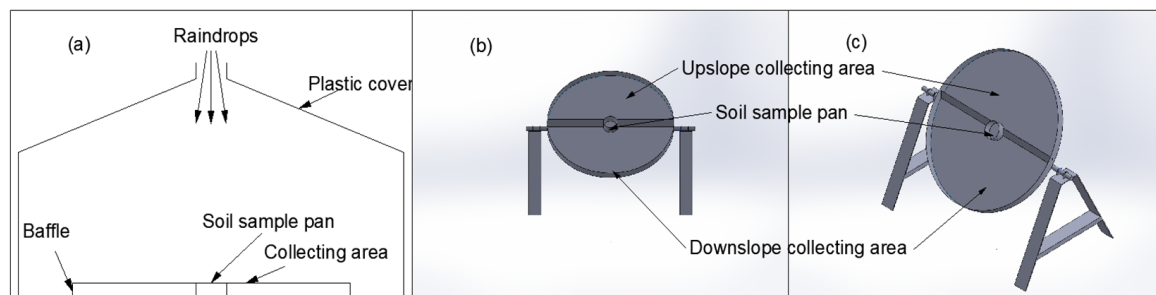


Figure 1. (a) An overview of the experimental setup. (b) Schematic of the front view of the splash pan. (c) Schematic of the side view of the splash pan.

2.3. Measurements and Calculations

Ten years of precipitations collected from a field experimental plot showed that the peak rainfall intensities of individual rainfall events ranged from 2.87 ~ 148.12 mm h^{-1} , and most erosion mainly occurs under high rainfall intensity. Therefore, five slopes (0° , 5° , 10° , 15° and 20°) and five rainfall intensities (60 , 84 , 106 , 132 and 156 mm h^{-1}) were selected. These levels were fully combined and replicated twice, for a total of 50 experiments. The rainfall duration (t) is 30 min.

2.3.1. Detachment Rate and Transport Rate

After each test, the splash particles were collected separately from the upslope and downslope compartments, then dried in an oven at 105°C for 8 h and weighed. The upslope (downslope) splash masses are the total amount of soil particles moving up (down) along the slope caused by raindrop splash. In this study, the total amount of soil particles collected in the upslope compartments was considered as the upslope splash mass (D_u); the total amount of soil particles collected in the downslope compartments was considered as the downslope splash mass (D_d). In this study, the detachment and transport masses were calculated as follows:

$$D = D_d + D_u \quad (1)$$

$$T = D_d - D_u \quad (2)$$

where D is the amount of detachment (g), T is the amount of transport (g). The detachment and transport rates are calculated as follows:

$$D_r = D / (t\pi r^2 \times 10^{-6}) \quad (3)$$

$$T_r = T / (t\pi r^2 \times 10^{-6}) \quad (4)$$

where D_r is the detachment rate ($\text{g} \cdot \text{m}^{-2} \text{ min}^{-1}$), T_r is the transport rate ($\text{g} \cdot \text{m}^{-2} \text{ min}^{-1}$), t is the rainfall duration (min) and r is the radius of the soil sample pan (mm).

2.3.2. Raindrop Diameter Measurement

The raindrop diameter was measured by the color spot method [40]. A 1:10 mixture of eosin and talcum powder (w/w basis) was painted on the medium-speed qualitative filter paper (diameter = 15 cm). When raindrops fell on the filter paper, each raindrop produced a color spot on the filter paper. The diameter of each raindrop is calculated from the measured diameter of the colored spots:

$$D_i = 0.356 \times d^{0.712} \quad (5)$$

where D_i is the diameter of the raindrop (mm), d is the diameter of the color spot (mm). The median raindrop size (D_{50}) is defined as the size of the raindrop that corresponds to 50% of the cumulative particle size distribution of the sample, based on the number of large and small raindrops formed on the filter paper.

2.3.3. Calculation of Raindrop Terminal Velocity

Assuming that the raindrops are globular, the mass of the raindrops is calculated as:

$$m = (\pi D_i^3 \times 10^{-6}) / 6 \quad (6)$$

where m is the mass of raindrop (kg), D_i is the diameter of raindrop (mm).

The terminal velocity of the raindrops in the windless condition is mainly determined by the size of the raindrops and is commonly calculated using the modified Shah Yuqing formula and the modified Newton formula [42].

$$V = \begin{cases} 0.496 \times 10^{\sqrt{28.320 + 6.524 \log(0.1 D_i) - \log(0.1 D_i)^2 - 3.665}} & D_i < 1.9 \text{ mm} \\ (17.20 - 0.884 D_i) \sqrt{0.1 D_i} & D_i > 1.9 \text{ mm} \end{cases} \quad (7)$$

where V is the terminal velocity of the raindrop (m s^{-1}), D_i is the diameter of the raindrop (mm).

2.3.4. Calculation of Rainfall Kinetic Energy

For a single raindrop, the kinetic energy is calculated as:

$$E_i = m_i V_i^2 / 2 \quad (8)$$

where E_i is the kinetic energy of a single raindrop (J), m_i is the mass of a single raindrop (kg), and V_i is the terminal velocity of the raindrop (m s^{-1}). Then, the kinetic energy of all raindrops is summed to get the kinetic energy of rainfall:

$$KE = \sum_{i=1}^n E_i \quad (9)$$

where KE is the total kinetic energy of the rainfall (J), n is the total number of raindrops.

2.3.5. Calculation of Contribution Rate

Calculation of the contribution of rainfall intensity and slope to the effects of detachment and transport can be carried out using the following equation [43].

$$\beta_i = b_i \sigma_{xi} / \sigma_y \quad (10)$$

$$P_i = (R^2 \beta_i^2 \times 100) / \sum_{i=1}^n \beta_i^2 \quad (11)$$

where P_i is the contribution of the i -th independent variable (%), R^2 is the coefficient of determination of the multiple regression equation, β_i is the standardized regression coefficient of the i -th independent variable, b_i is the regression coefficient of the i -th independent variable, σ_{xi} is the standard deviation of variable xi , σ_y is the standard deviation of variable y .

2.3.6. Data Analysis

The coefficient of determination (R^2), and the Nash–Sutcliffe Efficiency Index (NSE) [44] were used to evaluate the performance of empirical equations based on experimental data. Formulas for R^2 and NSE are as follows:

$$R^2 = [\sum_{i=1}^n (O_i - \bar{O})(P_i - \bar{P})]^2 / [\sum_{i=1}^n (O_i - \bar{O})^2 \sum_{i=1}^n (P_i - \bar{P})^2] \quad (12)$$

$$NSE = 1 - \frac{\sum (O_i - P_i)^2}{\sum (O_i - \bar{O}_i)^2} \quad (13)$$

where O_i are measured values, P_i are calculated values, \bar{O} is the mean of the measured values, and \bar{P} is the mean of the calculated values. NSE reflects the relative magnitude of the residual variance compared with the variance of the observed data [good ($NSE > 0.7$), satisfactory ($0.4 < NSE \leq 0.7$) and unsatisfactory ($NSE \leq 0.4$)].

3. Results and Discussion

3.1. Effects of the Rainfall Intensity and Slope on Splash Detachment and Transport

3.1.1. Effects of the Rainfall Intensity and the Slope on Detachment Rate

The variations in the detachment rate with rainfall intensity at the different slopes are shown in Figure 2. The overall trend in the detachment rate increased with increasing rainfall intensity at the different slopes. The detachment rate exhibited a negative correlation with the slope at a rainfall intensity lower than 108 mm h^{-1} , while a positive correlation was observed at a rainfall intensity higher than 108 mm h^{-1} . Table 1 summarizes the linear relationships between the detachment rate and rainfall intensity at the different slopes, with coefficient of determination (R^2) values ranging from 0.94–0.99, thus indicating significant correlations. Table 2 provides the equations for the relationships between the detachment rate and slope at the different rainfall intensities, with R^2 values ranging from 0.08–0.94.

With increasing rainfall intensity, the removal effect of raindrops on the soil surface increased, resulting in more soil particles being separated from the soil. Thus, the detachment rate generally increased with increasing rainfall intensity [9,10,24,25,32,45–52]. However, this increase was not uniform. At rainfall intensities higher than 84 mm h^{-1} , the detachment rate increase decreased for low slopes (0° , 5° and 10°). For high slopes (15° and 20°), the increase declined at rainfall intensities higher than 132 mm h^{-1} . The reason for this phenomenon may be that as the rainfall intensity is increased, the higher induced runoff constrains raindrop splash erosion. Therefore, when the rainfall intensity increases to a certain level, the detachment rate gradually decreases with increasing rainfall intensity [53,54]. With increasing slope, the runoff generated by rainfall spends relatively less time on the soil surface, and the constraint of the runoff depth on splash erosion decreases. Therefore, the inflection point at which the increase rate of detachment decreases at high slopes occurs relatively late [55].

The variations in the detachment rate with the slope exhibited an inflection point at a rainfall intensity of 108 mm h^{-1} . At a sloping angle, the rainfall-bearing region of the slope is the horizontal projected area. The steeper the slope is, the smaller the segment projection area and the less rainfall per unit area. The rain-bearing area on gentle slopes is larger than that on steep slopes, so the detachment rate on gentle slopes is higher [29,56–58]. However, simulated rainfall was supplied by a device in this, and the number of droplets increased but the size decreased at high rainfall intensities ($>108 \text{ mm h}^{-1}$) due to the pressure change, which is examined later. Although the rainfall intensity was increased, the droplet density decreased, resulting in reduced effects of the rainfall intensity and relatively enhanced effects of the slope on detachment [49,54,59–61]. The slope could affect the detachment rate because of the different raindrop impact angles. Raindrop impact gives way to a downslope drift on an inclined soil surface, and this drift produces a downslope bias in the lateral spreading of the drop associated with the downslope component of the incident impact velocity [33,34]. These reasons may lead to a significant increase in downslope detachment, which in turn affects total splash detachment. Therefore, at a rainfall intensity higher than 108 mm h^{-1} , the detachment rate was higher for high slopes than for low slopes. The effect of the slope on detachment is complex [28,53,54,62–64].

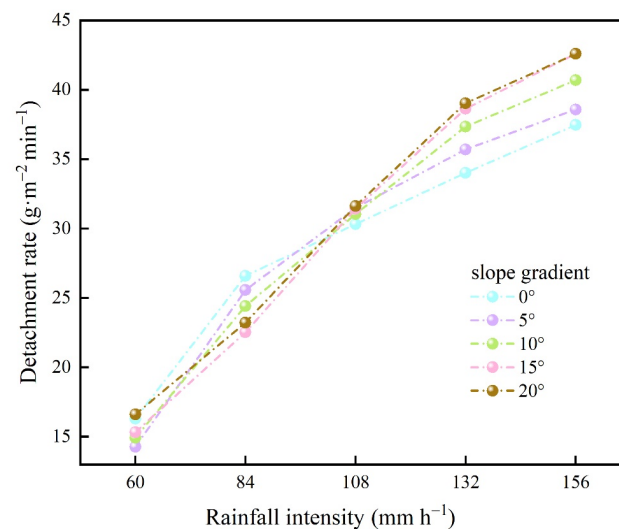


Figure 2. Variations of detachment rate with rainfall intensity under different slopes.

Table 1. Relationships between detachment rate (D_r , $\text{g} \cdot \text{m}^{-2} \cdot \text{min}^{-1}$) and rainfall intensity (I , mm h^{-1}).

Slope ($^{\circ}$)	Relationships between D_r and I	R^2
0	$D_r = 0.2074 I + 6.534$	0.94
5	$D_r = 0.2446 I + 2.7014$	0.93
10	$D_r = 0.2686 I + 0.6791$	0.97
15	$D_r = 0.2942 I - 1.6732$	0.99
20	$D_r = 0.2824 I + 0.113$	0.99

Table 2. Relationships between detachment rate (D_r , $\text{g} \cdot \text{m}^{-2} \cdot \text{min}^{-1}$) and slope (S , $^{\circ}$).

Rainfall Intensity (mm h^{-1})	Relationships between D_r and S	R^2
60	$D_r = 0.0335 S + 15.154$	0.08
84	$D_r = -0.1961 S + 26.426$	0.87
108	$D_r = 0.0517 S + 30.663$	0.59
132	$D_r = 0.2588 S + 34.358$	0.96
156	$D_r = 0.2848 S + 37.535$	0.94

3.1.2. Effects of the Rainfall Intensity and Slope on the Transport Rate

Figure 3 shows the variations in the transport rate with rainfall intensity at different slopes. In general, the transport rate exhibited an increasing trend with increasing rainfall intensity and slope. With increasing rainfall intensity, the increase rate remained more stable for low slopes (0° , 5° and 10°), and the increase rate was higher for high slopes (15° and 20°). Table 3 provides the linear equations for the relationships between the transport rate and rainfall intensity, with R^2 values ranging from 0.76–0.99. Table 4 provides the equations for the relationships between the transport rate and slope, with R^2 values ranging from 0.98 to 0.99.

The rainfall intensity provide the material basis and power supply for splash transport [15,16,36,50]. A higher rainfall intensity produces more loose soil particles, and more particles are transported along the slope due to raindrop strikes [2,59,65–70]. Therefore, the transport rates generally increase with increasing rainfall intensity [30,32,36,50–52,71,72]. An increasing slope could alter the striking angle and striking kinetic energy of raindrops on the soil surface. When soil particles move downslope, the kinetic energy component of raindrop striking and the raindrop gravity enhance the initial kinetic energy of soil particle movement, which facilitates the downslope movement of soil particles. When soil particles move upslope, gravity functions as a hindrance, which causes differences in the splashed mass between upslope and downslope regions [10,28,49,73]. Therefore, the transport rate increases with increasing slope [3,27,30,51,53,63,71,74]. The steeper the slope is, the more significant the tendency for particles to move downslope; thus, the transport rates increase more notably with increasing rainfall intensity under high-slope conditions [37,75,76].

The differences in splash mass between the upslope and downslope positions could also be represented by the ratio, as shown in Figure 4. The ratio significantly decreased with increasing slope, with values close to 1 at 0° and significantly lower than 1 at the other slopes. At 0° , the movement of splashed soil particles induced by raindrop striking is random, with equal chances of splashing upwards and downwards, so the ratio is close to 1. A ratio lower than 1 indicates that there is more splashing on the downslope than the upslope. The lower the ratio is, the larger the difference in splashing between the downslope and upslope regions, and the higher the transport rate. In other words, the transport rate increases with slope. The effect of the rainfall intensity on the transport rate is not as significant as that of the slope.

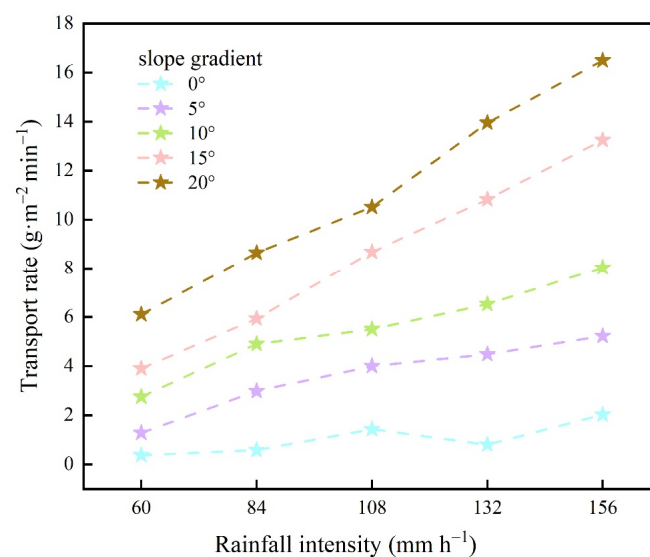


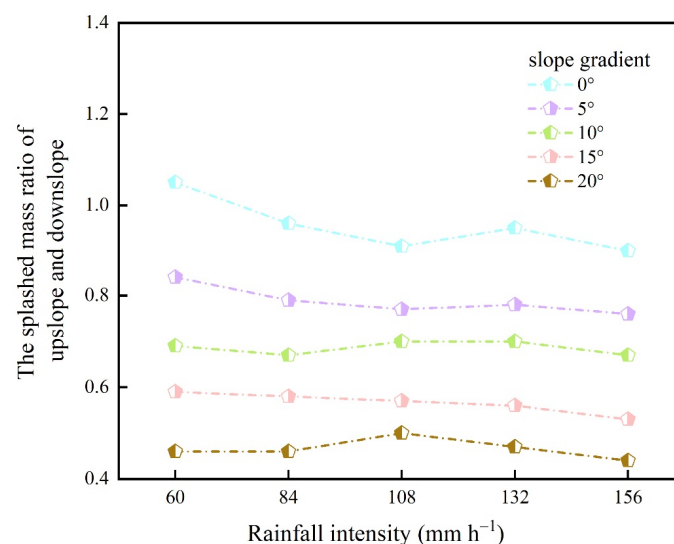
Figure 3. Variations of transport rate with rainfall intensity under different slopes.

Table 3. Relationships between transport rate (T_r , $\text{g}\cdot\text{m}^{-2}\text{ min}^{-1}$) and rainfall intensity (I , mm h^{-1}).

Slope ($^{\circ}$)	Relationships between T_r and I	R^2
0	$T_r = 0.0208 I - 1.3535$	0.76
5	$T_r = 0.0391 I - 0.6287$	0.93
10	$T_r = 0.0508 I + 0.0593$	0.96
15	$T_r = 0.0982 I - 2.0908$	0.99
20	$T_r = 0.1087 I - 0.6044$	0.99

Table 4. Relationships between transport rate (T_r , $\text{g}\cdot\text{m}^{-2}\text{ min}^{-1}$) and slope (S , $^{\circ}$).

Rainfall Intensity (mm h^{-1})	Relationships between T_r and S	R^2
60	$T_r = 0.3113 S - 0.3819$	0.99
84	$T_r = 0.3813 S + 0.7962$	0.98
108	$T_r = 0.4566 S + 1.4564$	0.99
132	$T_r = 0.6532 S + 0.7817$	0.99
156	$T_r = 0.7395 S + 1.606$	0.99

**Figure 4.** Variations of the splashed mass ratio of upslope and downslope with rainfall intensity under different slopes.

3.1.3. Contributions of the Rainfall Intensity and Slope to Detachment and Transport

The contributions of the rainfall intensity and slope to detachment were 94.77% and 0.46%, respectively. This result indicates that the detachment rate is influenced mainly by the rainfall intensity and that the slope imposes very little effect on the detachment rate. This suggests that detachment is more sensitive to the rainfall intensity than to the slope, and many studies have yielded similar conclusions [29,37,72,77,78].

The contributions of rainfall intensity and slope to the transport rate were 23.89% and 67.49%, respectively. The partial correlation coefficient between the transport rate and slope was higher than that between the transport rate and rainfall intensity, indicating that the transport rate is more sensitive to slope changes [54]. It has also been shown that the sediment transport variability always depends on the slope [30,79], which is consistent with the results of this study. However, it has been noted that the transport rate is more sensitive to the rainfall intensity than to the slope [36,37]. This difference in results may be due to variations in experimental design.

3.2. Rainfall Kinetic Energy

Particle detachment or transport during splash erosion is related to the number of raindrops striking the surface and the raindrop strike energy. The rainfall intensity is only a descriptive parameter of the number of raindrops received by soil particles, but does not represent the kinetic energy of raindrops. The rainfall intensity is influenced mainly by the raindrop size and raindrop terminal velocity. The kinetic energy of raindrops triggers soil erosion by breaking up and mobilizing soil particles, causing their splashing. The raindrop kinetic energy is the main factor contributing to the detachment of soil particles by splashing [80,81]; it is also the most appropriate way to express the erosive power of rainfall [82]. Therefore, the rainfall kinetic energy must also be considered when examining the influence of rainfall on splash erosion.

The variations in D_{50} , V , and KE with I are listed in Table 5. D_{50} , V , and KE all increased with increasing rainfall intensity at a rainfall intensity ranging from 60–108 mm h^{−1}. However, when the kinetic energy increased to a certain value, D_{50} , V , and KE no longer increased with increasing rainfall intensity. This value was even lower than that corresponding to the minimum rainfall intensity of 60 mm h^{−1} during the period when the rainfall intensity was increased from 132–156 mm h^{−1}.

Table 5. Variations of D_{50} , V and KE with I .

I (mm/h)	D_{50} (mm)	V (m/s)	KE (J)
60	1.83	6.65	7.09×10^{-6}
84	1.89	6.83	8.24×10^{-6}
108	1.96	6.88	9.34×10^{-6}
132	1.7	6.25	5.02×10^{-6}
156	1.68	6.19	4.75×10^{-6}

This phenomenon may be caused by the nozzles of the rainfall simulator, in which different droplet sizes can produce the same rainfall intensity. For the simulated rainfall device to achieve high rainfall intensities, the system increases the pressure on the nozzle and thus emits a larger number of smaller droplets than before. The droplet size is small, but the number of droplets is sufficiently large enough [82–84] to achieve the rainfall intensity set by the system. This differs from the natural phenomenon of larger droplets occurring at higher rainfall intensities [85]. As droplet sizes vary, the decrease rates differ, producing different kinetic energy levels. A few large droplets exhibit high kinetic energy, while many small droplets exhibit low kinetic energy [45]. This suggests that even a relatively low rainfall intensity could produce high kinetic energy, which is consistent with the findings of other researchers [64,86–88].

Both the rainfall intensity and kinetic energy of raindrops are parameters that describe the rainfall characteristics. The rainfall intensity is a parameter that describes the number of raindrops received by soil particles, and the kinetic energy of rainfall is a parameter that describes the splash energy of raindrops. In Table 5, the kinetic energy, median particle size and terminal velocity exhibit different trends from that in the rainfall intensity. Therefore, when modelling detachment and transport, it is important to consider the rainfall intensity and other physical rainfall parameters, such as kinetic energy, rather than directly considering a single rainfall characteristic only.

3.3. Key Parameter Selections for Splash Detachment and Transport

As indicated in Table 6, there was a significant correlation between the detachment rate (D_r) and I , D_{50} , V , and KE , but not between the detachment rate and slope. Therefore, the slope was not considered in the detachment model. There were significant correlations between the transport rate (T_r) and I and S . However, there were no statistically significant correlations between D_{50} , V , or KE . This may be due to the very small range of droplet sizes, i.e., 1.68 mm–1.96 mm. This represents only a 15% difference between the largest and

smallest raindrops. The difference between the maximum and minimum drop velocities was even smaller, at approximately 11%. Therefore, only the rainfall intensity and slope factors were considered in the transport model.

Table 6. Pearson correlation analysis between I , S , D_{50} , V , KE and D_r , T_r .

Parameter	D_r		T_r	
	r	p	r	p
I	0.973	<0.01	0.489	<0.05
S	0.068	>0.05	0.822	<0.01
D_{50}	−0.546	<0.01	−0.302	>0.05
V	−0.642	<0.01	−0.346	>0.05
KE	−0.529	<0.01	−0.293	>0.05

3.4. Splash Detachment Equation and Transport Equation

3.4.1. Splash Detachment Equation

Since D_{50} , V and KE exhibited different trends from I , multiple regression analysis was used to analyze the combined response of the detachment rate to I and D_{50} , V , and KE . The combined effects of the number of raindrops and raindrop energy on detachment were modelled as follows:

$$D_r = 0.1153 I^{1.09} D_{50}^{0.79} (R^2 = 0.99, NSE = 0.98, p < 0.01) \quad (14)$$

$$D_r = 0.0162 I^{1.11} V^{1.22} (R^2 = 0.99, NSE = 0.99, p < 0.01) \quad (15)$$

$$D_r = 0.0813 I^{1.10} KE^{0.18} (R^2 = 0.99, NSE = 0.99, p < 0.01) \quad (16)$$

The estimated D_r using Equations (14)–(16) satisfactorily matched the measured D_r with R^2 of 0.99, and NSE of 0.98, 0.99, 0.99, respectively. Figure 5 shows favorable agreement between the calculated and measured detachment rates. The detachment rate showed a power function relationship with I and D_{50} , V , and KE . The exponent of the rainfall intensity remained at a consistent level of approximately 1.10. The D_{50} exponent in this model was smaller than the I exponent. Several scholars have reported similar conclusions: the D_{50} exponent is 0.545, and the I exponent is 0.913 [11]. However, other scholars have established models in which the raindrop diameter exponent is greater than the rainfall intensity exponent [4]. The V exponent in the model developed in this experiment is greater than the I exponent, and similar conclusions have been reached by scholars suggesting that detachment is proportional to the 4.33rd power of the velocity and 0.65th power of the intensity [5]. The exponent of KE in the model established in this experiment is smaller than that of I , but the opposite conclusion has been obtained by other researchers [22,30,89,90]. This may occur because only three raindrop diameters were simulated in previous experiments using syringes, where low rainfall intensities were related to small raindrops, and high rainfall intensities were related to large raindrops. Large raindrops correspond to a higher rainfall kinetic energy. In contrast, in this experiment, the rainfall simulator ejected more but smaller droplets at higher rainfall intensities. The exponents of the established detachment model differ from those in studies, probably due to differences in the soil type and experimental design, so further research is warranted for splash detachment of loess.

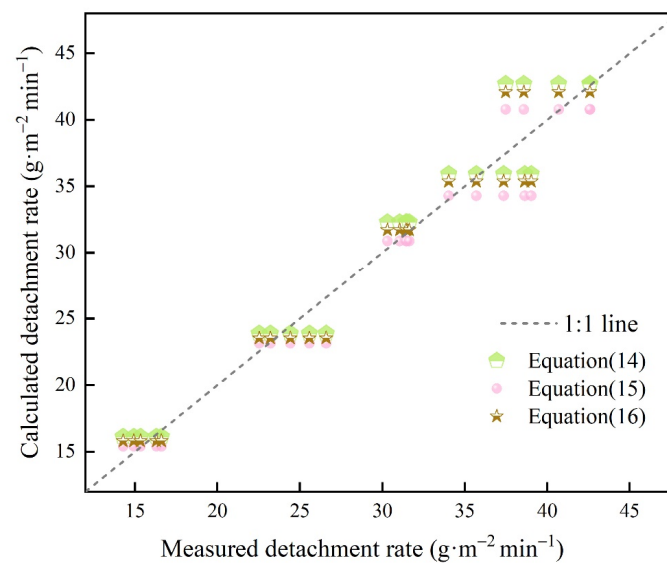


Figure 5. Measured vs. calculated detachment rate (D_r) (using Equations (14)–(16)).

3.4.2. Splash Transport Equation

Multiple regression analysis was employed to analyze the response of the transport rate to the rainfall intensity and slope, and the following equation was obtained:

$$T_r = 0.0973 I^{0.33} S^{1.14} \quad (R^2 = 0.83, NSE = 0.76, p < 0.01) \quad (17)$$

$$T_r = 0.00657 I^{1.343} S^{0.116} \quad (R^2 = 0.914, NSE = 0.874, p < 0.01) \quad (18)$$

$$T_r = 0.00218 I^{1.165} S^{1.033} \quad (R^2 = 0.986, NSE = 0.986, p < 0.01) \quad (19)$$

The estimated T_r using Equation (17) matched the measured T_r with $R^2 = 0.83$, and $NSE = 0.76$, but shows a significant number of outliers (Figure 6). From Figure 3 and Table 4, there is a relationship switch between 10° and 15° (from nonlinear to a more linear). To exclude these inconsistencies, multiple regression analysis was conducted in two groups, and Equations (18) (0° , 5° and 10°) and (19) (15° and 20°) were obtained. The estimated T_r using Equations (18) and (19) matched the measured T_r well, and the data points were all distributed closely to the 1:1 line, indicating satisfactory fitting results. In this study, a power function of the rainfall intensity and slope was developed to estimate the effects of the rainfall intensity and slope on the transport rate during splash erosion. In terms of exponents, splash transport was more sensitive to an increase in the slope. The slope exponent is 0.116 at slopes below 10° , and 1.033 at slopes of 15° and 20° , indicating that the effect of the slope is accentuated when the slope is increased to more than 10° . Transport heavily depends on the asymmetry in splashed particles between downslope and upslope directions. This effect is primarily due to the radial variation in the surface-parallel momentum of the spreading raindrop; as a result, surface-parallel transport increases approximately linearly with slope [33,34]. Regarding the relationship between splash transport and slope, several scholars have proposed slope exponents ranging from 1.0 to 2.0 [91], while others have obtained slope exponents of 0.75 and 1.37 [92,93]. Another model was developed with an exponent for the slope of 0.865 [36], which was modified to 1.13 [94]; this value is very close to the slope index value in Equation (17). In terms of the relationship between transport and rainfall intensity, the squared value of the rainfall intensity can reasonably describe the variation in the transport rate [36,37]. However, the rainfall intensity exponent in the model developed by some authors is 0.99 [94], which is almost half the value of the previously developed model [36,37]. The transport of soil particles is related not only to raindrop characteristics but also soil properties. This difference in exponents may be due to differences in the test conditions and design as well as soil properties. Furthermore, the exponent ranges for the rainfall intensity and

slope were 1.0~1.8 and 0.9~1.8, respectively [74], but there is no convincing support for the exponent of one variable greatly exceeding that of the other. In our study, the slope, rather than the rainfall intensity, more significantly affects the transport rate under high slope values. This may therefore indicate that more attention should be given to soil particle transport on steep slopes in loess areas.

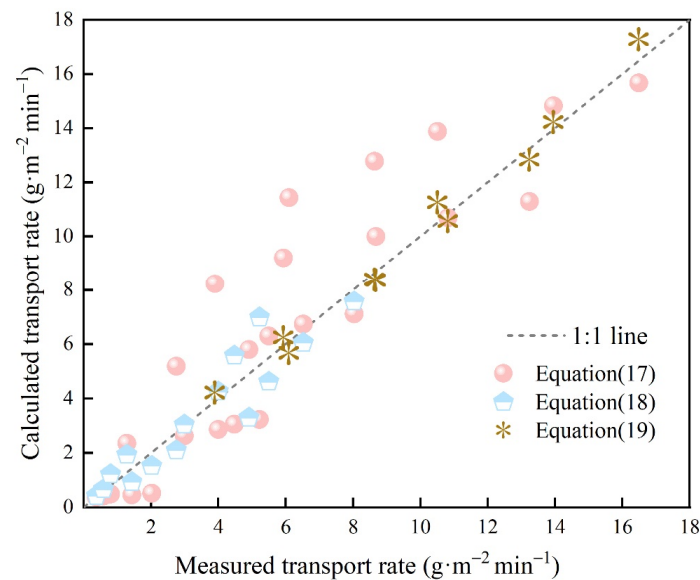


Figure 6. Measured vs. calculated transport rate (T_r) (using Equations (17)–(19)).

4. Conclusions

Relatively little splash transport modelling has been performed, especially regarding the quantitative contributions of rainfall and slope to detachment and transport, with no uniform conclusions. In this study, the effects of rainfall characteristics and slope on splash detachment and transport of soil particles on steep loess hillsides in China were studied under artificially simulated rainfall.

The rainfall intensity exerted a stronger positive effect on detachment than the slope considering linear equations. There were positive effects of either rainfall intensity or slope on the transport rates using linear equations. The rainfall intensity and slope contributed 94.77% and 0.46%, respectively, to the detachment rate and contributed 23.89% and 67.49%, respectively, to the transport rate. From a holistic viewpoint, the positive effects of slope became more visible on the detachment rate when the rainfall intensity exceeded 108 mm h^{-1} , and on the transport rate when the slope exceeded 15° . In this experiment, the rainfall kinetic energy (KE , J), raindrop median particle size (D_{50} , mm) and raindrop terminal velocity (V , m s^{-1}) increased with increasing rainfall intensity (I) within $60\text{--}108 \text{ mm h}^{-1}$, but then decreased with increasing rainfall intensity within the $132\text{--}156 \text{ mm h}^{-1}$ range, which was a result of the nozzles used in the simulations experiment. The rainfall intensity and raindrop kinetic energy characteristics ($D_{50}/V/KE$) were selected as ideal parameters for splash detachment (D_r , $\text{g}\cdot\text{m}^{-2} \text{ min}^{-1}$) modelling, while the rainfall intensity and slope were the key factors in splash transport (T_r , $\text{g}\cdot\text{m}^{-2} \text{ min}^{-1}$) modelling. The established splash detachment models are as follows: (1) $D_r = 0.1153 I^{1.09} D_{50}^{0.79}$ ($R^2 = 0.99$, $NSE = 0.98$, $p < 0.01$); (2) $D_r = 0.0162 I^{1.11} V^{1.22}$ ($R^2 = 0.99$, $NSE = 0.99$, $p < 0.01$); and (3) $D_r = 0.0813 I^{1.10} KE^{0.18}$ ($R^2 = 0.99$, $NSE = 0.99$, $p < 0.01$). The splash transport models are as follows: (1) $T_r = 0.00657 I^{1.343} S^{0.116}$ ($R^2 = 0.914$, $NSE = 0.874$, $p < 0.01$) (slopes of 0° , 5° and 10°) and (2) $T_r = 0.00218 I^{1.165} S^{1.033}$ ($R^2 = 0.986$, $NSE = 0.986$, $p < 0.01$) (slopes of 15° and 20°).

In summary, rainfall characteristics and slope notably influence the splash erosion process. Special consideration should be given to the effect of rainfall when studying splash detachment processes and to the effect of the slope when studying transport processes. Due to the different test conditions, the model developed in this paper must be validated in areas with different conditions and soil characteristics.

Author Contributions: Conceptualization, F.D., X.C. and J.L. Methodology, F.D., X.C., J.L., X.Q. and N.W. Investigation, J.L., F.D., X.Q., N.S., C.M. and Z.W. Writing—Original Draft, J.L., F.D. and X.C. Visualization, F.D., X.C., J.L. and X.Q. Writing—Reviewing, J.L., N.S., C.M. and Z.W. All authors have read and agreed to the published version of the manuscript.

Funding: This research was funded by the National Natural Science Foundation of China (42077058, 42377322, 41601282, 41867015), Young Talent fund of University Association for Science and Technology in Shaanxi, China (20210705), Fundamental Research Funds for Central Universities (GK202309005).

Institutional Review Board Statement: Not applicable.

Informed Consent Statement: Not applicable.

Data Availability Statement: Data used are published within the main body of the text and in the figures.

Acknowledgments: We gratefully acknowledge the assistance of the State Key Laboratory of Soil Erosion and Dryland Farming on the Loess Plateau in terms of test sites and equipment. The authors thank anonymous reviewers for insightful comments on the original manuscript.

Conflicts of Interest: The authors declare no conflicts of interest.

References

1. Lal, R. Soil erosion impact on agronomic productivity and environment quality. *Crit. Rev. Plant Sci.* **1998**, *17*, 319–464. [\[CrossRef\]](#)
2. Kinnell, P.I.A. Raindrop impact induced erosion processes and prediction: A review. *Hydrol. Process.* **2005**, *19*, 2815–2844. [\[CrossRef\]](#)
3. Ali, M.; Sterk, G.; Seeger, M.; Boersema, M.P.; Peters, P. Effect of hydraulic parameters on sediment transport capacity in overland flow over erodible beds. *Hydrol. Earth Syst. Sci.* **2012**, *16*, 591–601. [\[CrossRef\]](#)
4. Ellison, W.D. Studies of raindrop erosion. *Agric. Eng.* **1944**, *25*, 131–136.
5. Ellison, W.D. Soil erosion studies. *Agric. Eng.* **1947**, *28*, 145–146.
6. Legout, C.; Leguedois, S.; Bissonnais, Y.L.; Issa, O.M. Splash distance and size distributions for various soils. *Geoderma* **2005**, *124*, 279–292. [\[CrossRef\]](#)
7. Foster, G.R.; Meyer, L.D.; Onstad, C.A. An erosion equation derived from basic erosion principles. *Trans. ASAE* **1977**, *20*, 678–682. [\[CrossRef\]](#)
8. Hairsine, P.B.; Rose, C.W. Rainfall detachment and deposition: Sediment transport in the absence of flow-driven processes. *Soil Sci. Soc. Am. J.* **1991**, *55*, 320–324. [\[CrossRef\]](#)
9. Angulo-Martínez, M.; Beguería, S.; Navas, A.; Machin, J. Splash erosion under natural rainfall on three soil types in NE Spain. *Geomorphology* **2012**, *175*, 38–44. [\[CrossRef\]](#)
10. Wu, J.; Zhao, L.S.; Wu, Q.; Li, Z.B. The role of surface microreliefs in influencing splash erosion: A laboratory study. *Soil Water Res.* **2016**, *11*, 83–89. [\[CrossRef\]](#)
11. Fu, Y.; Yang, M.X.; Li, G.L.; Wang, D.; Zheng, T.H. Selectivity of aggregate fractions for loess soils under different raindrop diameters. *J. Soils Sediments* **2021**, *21*, 189–202. [\[CrossRef\]](#)
12. Sobol, N.V.; Gabbasova, I.M.; Komissarov, M.A. Effect of rainfall intensity and slope steepness on the development of soil erosion in the Southern Cis-Ural region (A model experiment). *Eurasian Soil Sci.* **2017**, *50*, 1098–1104. [\[CrossRef\]](#)
13. Wischmeier, W.H.; Smith, D.D. A universal soil-loss equation to guide conservation farm planning. *Trans. Int. Congr. Soil Sci.* **1960**, *1*, 418–425.
14. Al-Durrah, M.; Bradford, J.M. New methods of studying soil detachment due to waterdrop impact. *Soil Sci. Soc. Am. J.* **1981**, *45*, 949–953. [\[CrossRef\]](#)
15. Laws, J.O.; Pasron, D.A. The relationship of raindrop size to intensity. *Trans. Amer. Geophys. Union* **1943**, *24*, 248–262. [\[CrossRef\]](#)
16. Martínez-Mena, M.; Castillo, V.; Albaladejo, J. Relations between interrill erosion processes and sediment particle size distribution in a semiarid Mediterranean area of SE of Spain. *Geomorphology* **2002**, *45*, 261–275. [\[CrossRef\]](#)
17. Dunne, T.; Zhang, W.H.; Aubry, B.F. Effects of rainfall, vegetation, and microtopography on infiltration and runoff. *Water Resour. Res.* **1991**, *27*, 2271–2285. [\[CrossRef\]](#)
18. Meyer, L.D.; Harmon, W.C. How row-sideslope length and steepness affect sideslope erosion. *Trans. ASAE* **1989**, *32*, 639–644. [\[CrossRef\]](#)

19. Ben-Hur, M.; Agassi, M. Predicting interrill erodibility factor from measured infiltration rate. *Water Resour. Res.* **1997**, *33*, 2409–2415. [\[CrossRef\]](#)
20. Komatsu, H.; Shinohara, Y.; Kume, T.; Otsuki, K. Changes in peak flow with decreased forestry practices: Analysis using watershed runoff data. *J. Environ. Manag.* **2011**, *92*, 1528–1536. [\[CrossRef\]](#)
21. Ries, J.B.; Marzen, M.; Iserloh, T.; Fister, W. Soil erosion in Mediterranean landscapes-experimental investigation on crusted surfaces by means of the portable wind and rainfall simulator. *J. Arid. Environ.* **2014**, *100*, 42–51. [\[CrossRef\]](#)
22. Bubenzer, G.D.; Jones, B.A. Drop size and impact velocity effects on the detachment of soil under simulated rainfall. *Trans. ASAE* **1971**, *14*, 625–628. [\[CrossRef\]](#)
23. Park, S.W.; Mitchell, J.K.; Bubenzer, G.D. Rainfall characteristics and their relation to splash erosion. *Trans. ASAE* **1983**, *26*, 795–804. [\[CrossRef\]](#)
24. Liu, T.; Luo, J.; Zheng, Z.C.; Li, T.X.; He, A.Q. Effects of rainfall intensity on splash erosion and its spatial distribution under maize canopy. *Nat. Hazards* **2016**, *84*, 233–247. [\[CrossRef\]](#)
25. Zumr, D.; Mutzenberg, D.V.; Neumann, M.; Jeřábek, J.; Laburda, T.; Kavka, P.; Johannsen, L.L.; Zambon, N.; Klik, A.; Strauss, P.; et al. Experimental Setup for splash erosion monitoring-study of silty loam splash characteristics. *Sustainability* **2020**, *12*, 157. [\[CrossRef\]](#)
26. Wu, P.T.; Zhou, P.H. The impact of surface slope on raindrop splash erosion. *Bull Soil Water Conserv.* **1991**, *11*, 8–13, 28. (In Chinese)
27. Wan, Y.; El-Swaify, S.A.; Sutherland, R.A. Partitioning interrill splash and wash dynamics: A novel laboratory approach. *Soil Technology* **1996**, *9*, 55–69. [\[CrossRef\]](#)
28. Fu, S.; Liu, B.; Liu, H.; Xu, L. The effect of slope on interrill erosion at short slopes. *Catena* **2011**, *84*, 29–34. [\[CrossRef\]](#)
29. Wu, B.; Wang, Z.; Zhang, Q.; Shen, N.; Liu, J. Evaluating and modelling splash detachment capacity based on laboratory experiments. *Catena* **2019**, *176*, 189–196. [\[CrossRef\]](#)
30. Quansah, C. The effect of soil type, slope, rain intensity and their interactions on splash detachment and transport. *Eur. J. Soil. Sci.* **1981**, *32*, 215–224. [\[CrossRef\]](#)
31. Scholten, T.; Geibler, C.; Goc, J.; Kühn, P.; Wiegand, C. A new splash cup to measure the kinetic energy of rainfalls. *J. Plant Nutr. Soil Sci.* **2011**, *174*, 596–601. [\[CrossRef\]](#)
32. Hu, W.; Zheng, F.L.; Bian, F. The directional components of splash erosion at different raindrop kinetic energy in the Chinese Mollisol Region. *Soil Sci. Soc. Am. J.* **2016**, *80*, 1329–1340. [\[CrossRef\]](#)
33. Furbish, D.J.; Childs, E.M.; Haff, P.K.; Schmeeckle, M.W. Rain splash of soil grains as a stochastic advection-dispersion process, with implications for desert plant-soil interactions and land-surface evolution. *J. Geophys. Res.* **2009**, *114*, F00A03. [\[CrossRef\]](#)
34. Furbish, D.J.; Hamner, K.K.; Schmeeckle, M.; Borosund, M.N.; Mudd, S.M. Rain splash of dry sand revealed by high-speed imaging and sticky paper splash targets. *J. Geophys. Res.* **2007**, *112*, F01001. [\[CrossRef\]](#)
35. Walker, P.H.; Kinnell, P.; Green, P. Transport of a noncohesive sandy mixture in rainfall and runoff experiments. *Soil Sci. Soc. Am. J.* **1978**, *42*, 793–801. [\[CrossRef\]](#)
36. Guy, B.T.; Dickinson, W.T.; Rudra, R.P. The roles of rainfall and runoff in the sediment transport capacity of interrill flow. *Trans. ASAE* **1987**, *30*, 1378–1386. [\[CrossRef\]](#)
37. Zhang, Q.; Wang, Z.; Wu, B.; Shen, N.; Liu, J. Identifying sediment transport capacity of raindrop impacted overland flow within transport-limited system of interrill erosion processes on steep loess hillslopes of China. *Soil Tillage Res.* **2018**, *187*, 109–117. [\[CrossRef\]](#)
38. Liu, J.E.; Wang, Z.L.; Yang, X.M.; Jiao, N.; Shen, N.; Ji, P.F. The impact of natural polymer derivatives on sheet erosion on experimental loess hillslope. *Soil Tillage Res.* **2014**, *139*, 23–27. [\[CrossRef\]](#)
39. Wu, Q.X.; Zhao, H.Y. Soil and water conservation objectives and countermeasures in the Loess Plateau. *Soil Water Conserv. Res.* **1996**, *6*, 76–80.
40. Dou, B.Z.; Zhou, P.H. Method of measure and mathematics to raindrop. *Bull Soil Water Conserv.* **1982**, *2*, 44–47. (In Chinese) [\[CrossRef\]](#)
41. Morgan, R.P.C. Field Studies of Rainsplash Erosion. *Earth SurFace Process.* **1978**, *3*, 295–298. [\[CrossRef\]](#)
42. Laws, J.O. Measurements of the fall-velocity of water-drops and raindrops. *Eos. Trans. Amer. Geophys. Union* **1941**, *22*, 709–721. [\[CrossRef\]](#)
43. Holrott, H.N. *Agricultural Production Effect Forecast*; Tan, J.W.; Liu, T.F., Translators; Agriculture Press: Beijing, China, 1983.
44. Nash, J.E.; Sutcliffe, J.V. River flow forecasting through conceptual models 1: A discussion of principles. *J. Hydrol.* **1970**, *10*, 282–290. [\[CrossRef\]](#)
45. Fernández-Raga, M.; Fraile, R.; Keizer, J.J. The kinetic energy of rain measured with an optical disdrometer: An application to splash erosion. *Atmos. Res.* **2010**, *96*, 225–240. [\[CrossRef\]](#)
46. Boroghani, M.; Hayavi, F.; Noor, H. Affectability of splash erosion by polyacrylamide application and rainfall intensity. *Soil Water Res.* **2012**, *7*, 159–165. [\[CrossRef\]](#)
47. Geißler, C.; Kühn, P.; Böhnke, M.; Bruelheide, H.; Shi, X.; Scholten, T. Splash erosion potential under tree canopies in sub-tropical SE China. *Catena* **2012**, *91*, 85–93. [\[CrossRef\]](#)
48. Begueria, S.; Angulo-Martinez, M.; Gaspar, L.; Navas, A. Detachment of soil organic carbon by rainfall splash: Experimental assessment on three agricultural soils of Spain. *Geoderma* **2015**, *245*, 21–30. [\[CrossRef\]](#)

49. Saedi, T.; Shorafa, M.; Gorji, M.; Moghadam, B.K. Indirect and direct effects of soil properties on soil splash erosion rate in calcareous soils of the central Zagross, Iran: A laboratory study. *Geoderma* **2016**, *271*, 1–9. [\[CrossRef\]](#)
50. Zhang, X.C.; Wang, Z.L. Interrill soil erosion processes on steep slopes. *J. Hydrol.* **2017**, *548*, 652–664. [\[CrossRef\]](#)
51. Wu, B.; Wang, Z.; Zhang, Q.; Shen, N. Distinguishing transport-limited and detachment-limited processes of interrill erosion on steep slopes in the Chinese loessial region. *Soil Tillage Res.* **2018**, *177*, 88–96. [\[CrossRef\]](#)
52. Yao, J.J.; Cheng, J.H.; Zhou, Z.D.; Sun, L.; Zhang, H.J. Effects of herbaceous vegetation coverage and rainfall intensity on splash characteristics in northern China. *Catena* **2018**, *167*, 411–421. [\[CrossRef\]](#)
53. Ghahramani, A.; Ishikawa, Y.; Gomi, T.; Miyata, S. Downslope soil detachment-transport on steep slopes via rain splash. *Hydrol. Process* **2011**, *25*, 2471–2480. [\[CrossRef\]](#)
54. Liu, W.J.; Luo, Q.P.; Li, J.T.; Wang, P.Y.; Lu, H.J.; Liu, W.Y.; Li, H.M. The effects of conversion of tropical rainforest to rubber plantation on splash erosion in Xishuangbanna, SW China. *Hydrol. Res.* **2015**, *46*, 168–174. [\[CrossRef\]](#)
55. Ma, B.; Yu, X.D.; Ma, F.; Li, Z.; Wu, F. Effects of crop canopies on rain splash detachment. *PLoS ONE* **2014**, *9*, e99717. [\[CrossRef\]](#)
56. Janeau, J.L.; Bricquet, J.P.; Planchon, O.; Valentin, C. Soil crusting and infiltration on steep slopes in northern Thailand. *Eur. J. Soil Sci.* **2003**, *54*, 543–553. [\[CrossRef\]](#)
57. Mouzai, L.; Bouhade, M. Shear strength of compacted soil: Effects on splash erosion by single water drops. *Earth Surf. Process. Landf.* **2011**, *36*, 7–96. [\[CrossRef\]](#)
58. Liu, W.J.; Liu, W.Y.; Lu, H.J.; Duan, W.P.; Li, H.M. Runoff generation in small catchments under a native rainforest and a rubber plantation in Xishuangbanna, SW China. *Water Environ. J.* **2011**, *25*, 138–147. [\[CrossRef\]](#)
59. Yuan, Z.; Chu, Y.; Shen, Y. Simulation of surface runoff and sediment yield under different land-use in a Taihang Mountains watershed, North China. *Soil Tillage Res.* **2015**, *153*, 7–19. [\[CrossRef\]](#)
60. Mahmoodabadi, M.; Sajjadi, S.A. Effects of rain intensity, slope gradient and particle size distribution on the relative contributions of splash and wash loads to rain-induced erosion. *Geomorphology* **2016**, *253*, 159–167. [\[CrossRef\]](#)
61. Nazir, R.; Ghareh, S.; Mosallanezhad, M.; Moayedi, H. The influence of rainfall intensity on soil loss mass from cellular confined slopes. *Measurement* **2016**, *81*, 13–25. [\[CrossRef\]](#)
62. Mizugaki, S.; Nanko, K.; Onda, Y. The effect of slope angle on splash detachment in an unmanaged Japanese cypress plantation forest. *Hydrol. Process* **2010**, *24*, 576–587. [\[CrossRef\]](#)
63. Defersha, M.B.; Quraishi, S.; Melesse, A. The effect of slope steepness and antecedent moisture content on interrill erosion, runoff and sediment size distribution in the highlands of Ethiopia. *Hydrol. Earth Syst. Sci.* **2011**, *15*, 2367–2375. [\[CrossRef\]](#)
64. Iserloh, T.; Ries, J.B.; Cerdà, A.; Echeverría, M.T.; Fister, W.; Geißler, C.; Kuhn, N.J.; Leon, F.J.; Peters, P.; Schindewolf, M.; et al. Comparative measurements with seven rainfall simulators on uniform bare fallow land. *Z. Geomorphol.* **2012**, *57*, 11–26. [\[CrossRef\]](#)
65. Kinnell, P.I.A. The effect of flow depth on sediment transport induced by raindrops impacting shallow flows. *Trans. ASAE* **1991**, *34*, 161–168. [\[CrossRef\]](#)
66. Kinnell, P.I.A. Interrill erodibilities based on the rainfall intensity flow discharge erosivity factor. *Soil Res.* **1993**, *31*, 319–332. [\[CrossRef\]](#)
67. Parsons, A.J.; Gadian, A.M. Uncertainty in modeling the detachment of soil by rainfall. *Earth Sur. Process. Landf.* **2000**, *25*, 723–728. [\[CrossRef\]](#)
68. Salles, C.; Poesen, J.; Govers, G. Statistical and physical analysis of soil detachment by rainfall impact: Rain erosivity indices and threshold energy. *Water Resour. Res.* **2000**, *36*, 2721–2729. [\[CrossRef\]](#)
69. Jayawardena, A.W.; Rezaur, R.B. Measuring drop size distribution and kinetic energy of rainfall using a force transducer. *Hydrol. Process.* **2000**, *14*, 37–49. [\[CrossRef\]](#)
70. Lim, Y.S.; Kim, J.K.; Kim, J.W.; Park, B.I.; Kim, M.S. Analysis of the relationship between the kinetic energy and intensity of rainfall in Daejeon, Korea. *Quat. Int.* **2015**, *384*, 107–117. [\[CrossRef\]](#)
71. Van, D.; Bruijnzeel, L.; Eisma, E.H. A methodology to study rain splash and wash processes under natural rainfall. *Hydrol. Process.* **2003**, *17*, 153–167. [\[CrossRef\]](#)
72. Wu, X.L.; Wei, Y.J.; Wang, J.G.; Xia, J.W.; Cai, C.F.; Wu, L.L.; Fu, Z.Y.; Wei, Z.Y. Effects of erosion degree and rainfall intensity on erosion processes for Ultisols derived from quaternary red clay. *Agric. Ecosyst. Environ.* **2017**, *249*, 226–236. [\[CrossRef\]](#)
73. Grismer, M. Standards vary in studies using rainfall simulators to evaluate erosion. *Calif. Agric.* **2012**, *66*, 102–107. [\[CrossRef\]](#)
74. Prosser, I.P.; Rustomji, P. Sediment transport capacity relations for overland flow. *Prog. Phys. Geog.* **2000**, *24*, 179–193. [\[CrossRef\]](#)
75. Cheng, J.H.; Qin, Y.; Zhang, H.J.; Cong, Y.; Yang, F.; Yan, Y.Q. Splash erosion under artificial rainfall in rocky mountain area of northern China. *T. Chin. Soc. Agric. Mach.* **2015**, *46*, 153–161.
76. Bako, A.N.; Cottenot, L.; Courtemanche, P.; Lucas, C.; James, F.; Darboux, F. Impacts of raindrops increase particle sedimentation in a sheet flow. *Earth Surf. Process. Landf.* **2022**, *47*, 1322–1332. [\[CrossRef\]](#)
77. Watson, D.A.; Lafen, J.M. Soil strength, slope, and rainfall intensity effects on interrill erosion. *Trans. ASAE* **1986**, *29*, 98–102. [\[CrossRef\]](#)
78. Shen, H.; Zheng, F.; Wen, L.; Han, Y.; Hu, W. Impacts of rainfall intensity and slope gradient on rill erosion processes at loessial hillslope. *Soil Tillage Res.* **2016**, *155*, 429–436. [\[CrossRef\]](#)
79. Zhao, Q.H.; Li, D.Q.; Zhuo, M.N.; Guo, T.L.; Liao, Y.S.; Xie, Z.Y. Effects of rainfall intensity and slope gradient on erosion characteristics of the red soil slope. *Stoch. Env. Res. Risk A* **2015**, *29*, 609–621. [\[CrossRef\]](#)

80. Wang, L.; Shi, Z.H.; Wang, J.; Fang, N.F.; Wu, G.L.; Zhang, H.Y. Rainfall kinetic energy controlling erosion processes and sediment sorting on steep hillslopes: A case study of clay loam soil from the Loess Plateau, China. *J. Hydrol.* **2014**, *512*, 168–176. [[CrossRef](#)]
81. Stocking, M.A.; Elwell, H.A. Rainfall erosivity over Rhodesia. *Trans. Inst. Br. Geogr.* **1976**, *1*, 231–245. [[CrossRef](#)]
82. Hudson, N.W. Raindrop size distribution in high intensity storms. *Rhod. J. Agric. Res* **1963**, *1*, 6–11.
83. Van Dijk, A.I.J.M.; Bruijnzeel, L.; Rosewell, C. Rainfall intensity–kinetic energy relationships: A critical literature appraisal. *J. Hydrol.* **2002**, *261*, 1–23. [[CrossRef](#)]
84. Goebes, P.; Seitz, S.; Geißler, C.; Lassu, T.; Peters, P.; Seeger, M.; Nadrowski, K.; Scholten, T. Momentum or kinetic energy—how do substrate properties influence the calculation of rainfall erosivity? *J. Hydrol.* **2014**, *517*, 310–316. [[CrossRef](#)]
85. Hamed, Y.; Albergel, J.; Pepin, Y.; Asseline, J.; Nasri, S.; Zante, P.; Berndtsson, R.; El-Niazy, M.; Balah, M. Comparison between rainfall simulator erosion and observed reservoir sedimentation in an erosion-sensitive semiarid catchment. *Catena* **2002**, *50*, 1–16. [[CrossRef](#)]
86. Cerdà, A.; Ibáñez, S.; Calvo, A. Design and operation of small and portable rainfall simulator for rugged terrain. *Soil Tech.* **1997**, *11*, 161–168. [[CrossRef](#)]
87. Mohamed, A.M.; Yasuda, H.; Salmi, A.; Anyoji, H. Characterization of rainfall generated by dripper-type rainfall simulator using piezoelectric transducers and its impact on splash soil erosion. *Earth Surf. Process Landf.* **2010**, *35*, 466–475. [[CrossRef](#)]
88. Petrú, J.; Kalibová, J. Measurement and computation of kinetic energy of simulated rainfall in comparison with natural rainfall. *Soil Water Res.* **2018**, *13*, 226–233. [[CrossRef](#)]
89. Free, G.R. Soil movement by raindrops. *Agric. Eng.* **1952**, *33*, 491–494, 496.
90. Free, G.R. Erosion characteristics of rainfall. *Agric. Eng.* **1960**, *41*, 447–449, 455.
91. Kirkby, M.J. Hillslope process-response models based on the continuity equation. *Slopes Form Process* **1971**, *3*, 15–30.
92. Moeyersons, J.; DePloey, J. Quantitative data on splash erosion simulated on unvegetated slopes. *Z. Geomorphol.* **1976**, *25*, 120–131.
93. Gabriels, D.; Pauwels, J.M.; Deboodt, M. The slope gradient as it affects the amount and size distribution of soil loss material from runoff on silt loam aggregates. Mededelingen Fakulteit Landbouwwetenschappen. *State Univ. Ghent.* **1975**, *40*, 1333–1338.
94. Rudra, R.P.; Guy, B.T.; Dickinson, W.T.; Sohrabi, T.M. Evaluating shallow overland flow sediment transport capacity mode. In Proceedings of the ASAE Annual Meeting. American Society of Agricultural and Biological Engineers 2007, Minneapolis, MI, USA, 17–20 June 2007; p. 1. [[CrossRef](#)]

Disclaimer/Publisher’s Note: The statements, opinions and data contained in all publications are solely those of the individual author(s) and contributor(s) and not of MDPI and/or the editor(s). MDPI and/or the editor(s) disclaim responsibility for any injury to people or property resulting from any ideas, methods, instructions or products referred to in the content.